Variants of Relativistic Coupled-cluster Method and their Implementation Challenges for Atomic Systems

Computational Atomic Structure (CompAS) meeting, 11-14 June 2025

B. K. Sahoo

Atomic, Molecular and Optical Physics Division
Physical Research Laboratory, Ahmedabad , India

प्लेटिनम जयंती
1947 75 2022
PLATINUM JUBILEE

PRL research encompasses the Earth, the Sun Immersed in the fields and radiations reaching from and to infinity, all that man's curiosity and intellect can reveal.

Founded in 1947 by Dr. Vikram A. Sarabhai, the Physical Research Laboratory (PRL) had a modest beginning at his residence, the RETREAT, with research on Cosmic Rays.

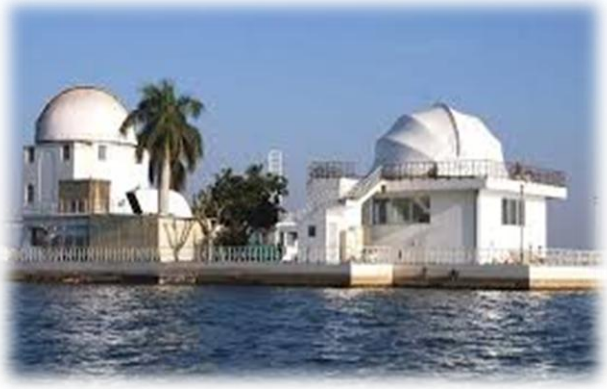

Ahmedabad, Gujarat, India

Area: 505 km²

Population: 79,22, 000

Ahmedabad, in western India, is the largest city in the state of Gujarat. The Sabarmati River runs through its center. On the western bank is the Gandhi Ashram at Sabarmati, which displays the spiritual leader's living quarters and artifacts. Across the river, the Calico Museum of Textiles, once a cloth merchant's mansion, has a significant collection of antique and modern fabrics.

Outline

- Our research interests
- General procedures of atomic calculations
- Coupled-cluster theory in spherical coordinate system
- Variants of coupled-cluster methods:
  - → **Bi-orthogonal approach**
  - → **Finite-field approach**
  - → **Expectation value evaluation approach**
  - → **Linear response approach**
  - → **Analytical response approach**
  - → **Fock-space approach**
  - → **Equation-of-motion approach**
- Results from our recent collaboration
- Summary and Outlook

High-precision Atomic Clocks

Wave

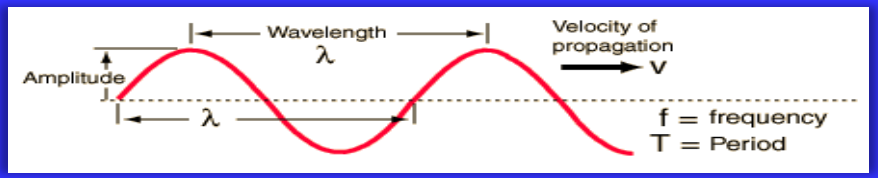

Time = No. of oscillations x Period

1 sec = Duration per oscillation = **1/f**

Atomic Systems (Atoms and Ions)

- Energy levels are fixed and reproducible.
- Transition frequency as clock.
- Long lifetime (narrow linewidth).
- Least affected by external fields.

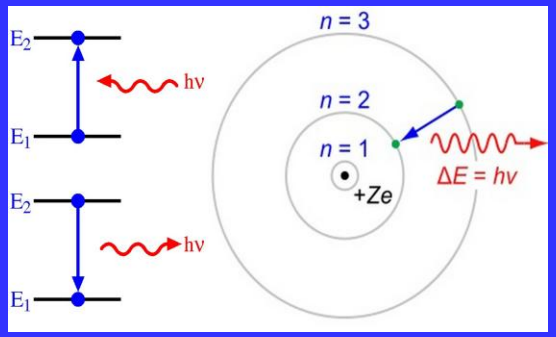

- Electronic levels (optical)
- Fine-structure (optical and THz)
- Hyperfine structure (microwave)

Role of Theoretical Study

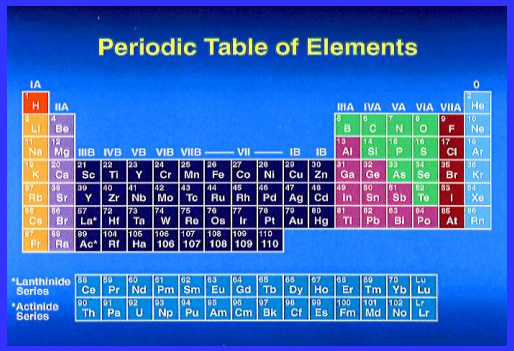

- Searching suitable transitions.
- Estimating black-body radiation shifts (multipolar).
- Electric field effects (laser).
- Magnetic field effects.

Applications:

1. Navigation, Geomapping
2. Volcanology
3. Constancy of fundamental constants (electron and proton masses), dark matter

Energy and Property Evaluation Equations

Schroedinger Eq: $H_0|\Psi_n\rangle = E_n|\Psi_n\rangle$

$$|\Psi\rangle = \frac{1}{\sqrt{N!}}\begin{bmatrix} |\psi_1(r_1\rangle & \cdots & |\psi_N(r_1)\rangle \\ \vdots & \ddots & \vdots \\ |\psi_1(r_N)\rangle & \cdots & |\psi_N(r_N)\rangle \end{bmatrix}$$

Property evaluation expression:

$$< O >_{fi} = \frac{\langle \Psi_f | O | \Psi_i \rangle}{\sqrt{\langle \Psi_f | \Psi_f \rangle \langle \Psi_i | \Psi_i \rangle}}$$

Isotope Shifts

nature physics LETTERS
https://doi.org/10.1038/s41567-020-01136-5
OPEN

Charge radii of exotic potassium isotopes challenge nuclear theory and the magic character of $N = 32$

Á. Koszorús[1,17], X. F. Yang[1,2], W. G. Jiang[3,4,5], S. J. Novario[3,4], S. W. Bai[2], J. Billowes[6], C. L. Binnersley[6], M. L. Bissell[6], T. E. Cocolios[1], B. S. Cooper[6], R. P. de Groote[7,8], A. Ekström[5], K. T. Flanagan[6,9], C. Forssén[5], S. Franchoo[10], R. F. Garcia Ruiz[11,12], F. P. Gustafsson[1], G. Hagen[4], G. R. Jansen[4], A. Kanellakopoulos[1], M. Kortelainen[7,8], W. Nazarewicz[13], G. Neyens[1,12], T. Papenbrock[3,4], P.-G. Reinhard[14], C. M. Ricketts[6], B. K. Sahoo[15], A. R. Vernon[1,6] and S. G. Wilkins[16]

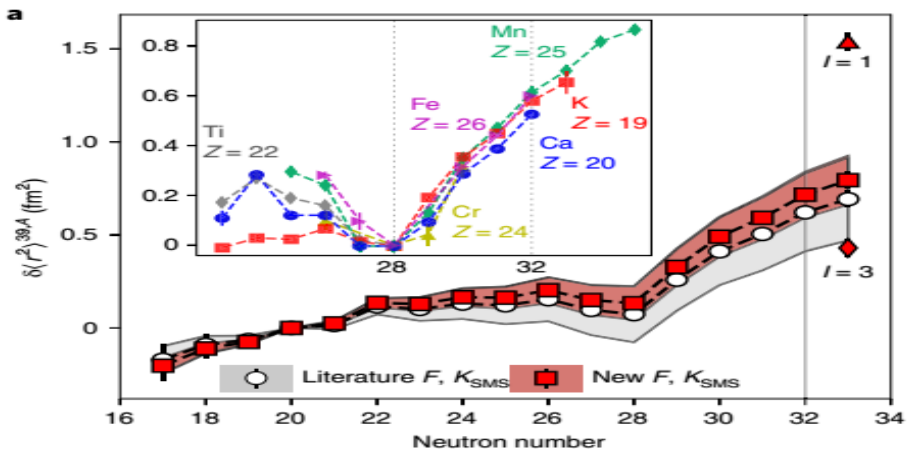

nature physics https://doi.org/10.1038/s41567-024-02612-y

Electromagnetic Properties of Indium Isotopes Elucidate the Doubly Magic Character of ^{100}Sn

Karthein J.[1,◇], Ricketts C.M.[2], Garcia Ruiz R.F.[1,2,3,†], Billowes J.[2], Binnersley C.L.[2], Cocolios T.E.[4], Dobaczewski J.[5,6], Farooq-Smith G.J.[4,*], Flanagan K.T.[2], Georgiev G.[7], Gins W.[4], de Groote R.P.[4], Gustafsson F.P.[4], Holt J.D.[8,9], Kanellakopoulos A.[4], Koszorús Á.[4], Leimbach D.[3,10], Lynch K.M.[2,3], Miyagi T.[11,12,13,6], Nazarewicz W.[14], Neyens G.[4], Reinhard P.-G.[15], Sahoo B.K.[16], Vernon A.R.[2], Wilkins S.G.[3,§], Yang X.F.[17], Yordanov D.T.[3,7]

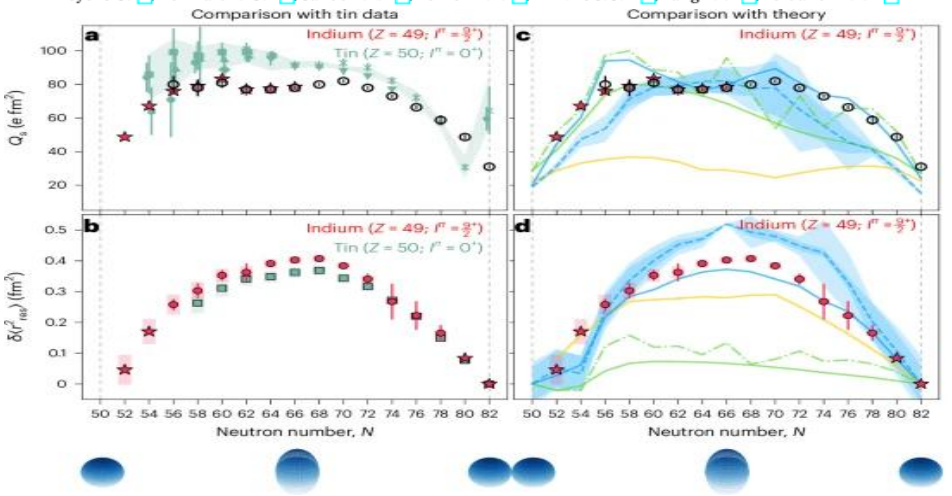

TABLE V. The inferred differential nuclear charge radii $\delta\langle r^2\rangle$ between isotopes A and A' ranging $168 - 176$ of Yb from the IS measurements in the α and β transitions (indicated with subscripts α and β) of Yb^+ [13]. The averaged values from both the transitions are recommended ($\delta\langle r^2\rangle_{\text{reco}}$) and are compared with the literature (Lit.) data.

(A, A')	$\delta\langle r^2\rangle_\alpha$	$\delta\langle r^2\rangle_\beta$	$\delta\langle r^2\rangle_{\text{reco}}$	Lit. [33]
(168, 170)	−0.1480	−0.1480	−0.1480(0)	−0.1561(3)
(170, 172)	−0.1391	−0.1390	−0.1391(1)	−0.1479(1)
(172, 174)	−0.1086	−0.1086	−0.1086(0)	−0.1207(1)
(174, 176)	−0.1036	−0.1036	−0.1036(0)	−0.1159(1)

- Gives precise values of nuclear charge radii of isotopes.
- Helps to describe nuclear structure (magic nuclei).
- Helps to validate nuclear theory.

Approaches to evaluate the first-order energy

In the perturbative theory: $|\Psi_n\rangle = |\Psi_n^{(0)}\rangle + \lambda|\Psi_n^{(1)}\rangle + \lambda^2|\Psi_n^{(2)}\rangle + \cdots$

$$E_n(\lambda) = E_n^{(0)} + \lambda E_n^{(1)} + \lambda^2 E_n^{(2)} + \cdots$$

$$\langle H_{int}\rangle \equiv E_{at}^{(1)} \approx \left.\frac{\partial E_\lambda}{\partial \lambda}\right|_{\lambda\to 0}$$

The expectation value evaluation (EVE) approach:

$$E_n^{(1)} = \langle H_{int}\rangle = \frac{\langle \Psi_n^{(0)}|H_{int}|\Psi_n^{(0)}\rangle}{\langle \Psi_n^{(0)}|\Psi_n^{(0)}\rangle}$$

Analytical Response (AR) approach:

$$\left(H_0 - E_n^{(0)}\right)|\Psi_n^{(1)}\rangle = \left(E_n^{(1)} - H_{int}\right)|\Psi_n^{(0)}\rangle$$

Objective: testing BSM physics

3 Fundamental Forces

12 Fundamental Fermions

12 Gauge Bosons

Parity violation

CP and T reversal violations

SU(2) X U(1)

CPT is conserved

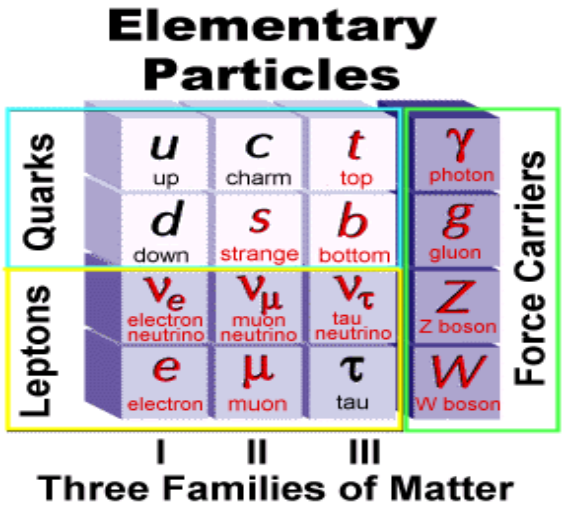

- Why three generations of particles?
- Sources of CP violation. (eg: matter-antimatter asymmetry)
- Explaining neutrino masses.
- And so on .....

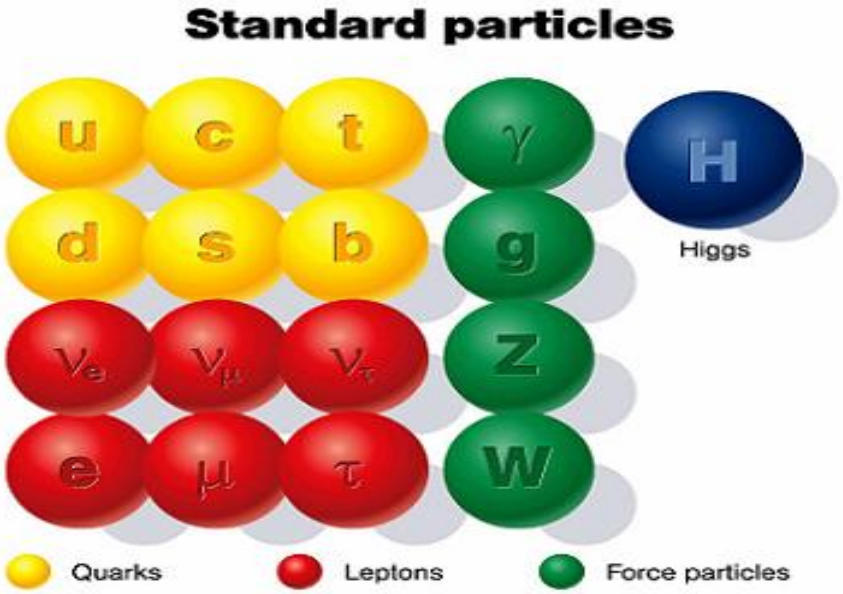

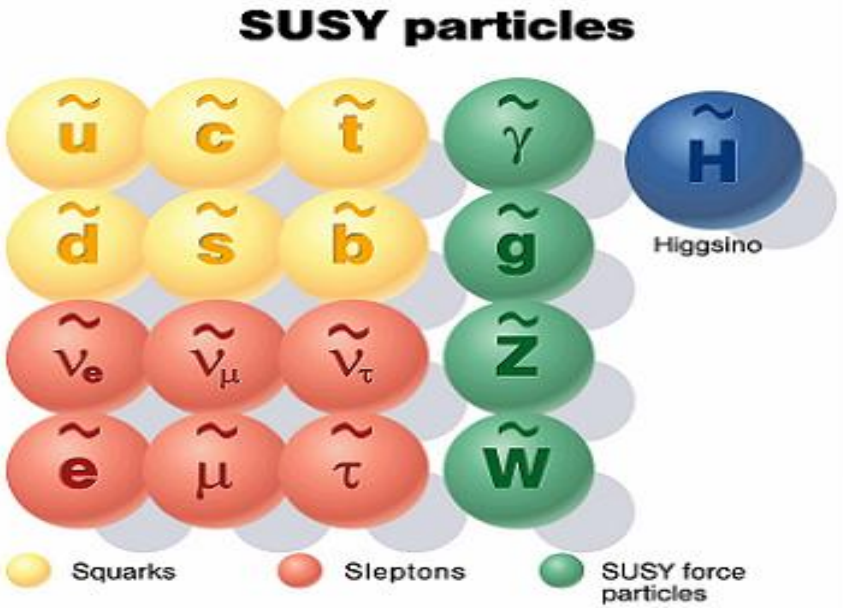

Atomic Parity Violation

6S →7S transition (Cs)

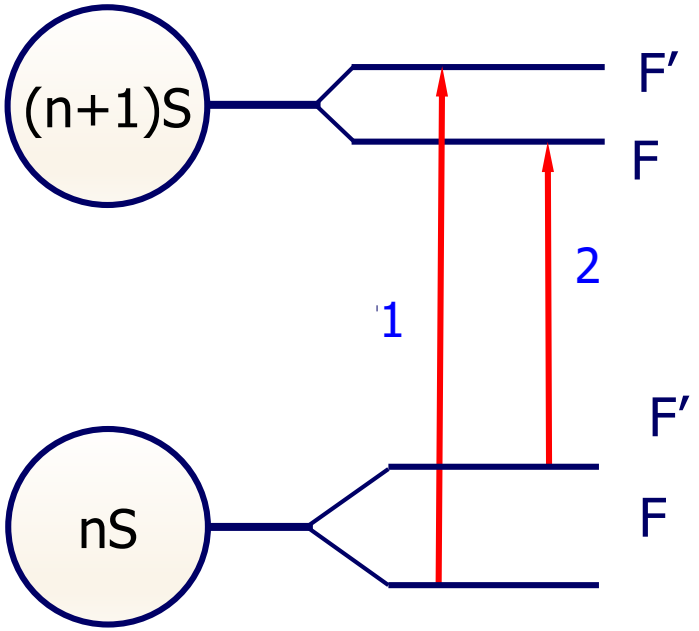

6S→5D$_{3/2,5/2}$ transitions (Cs/Ba$^+$)

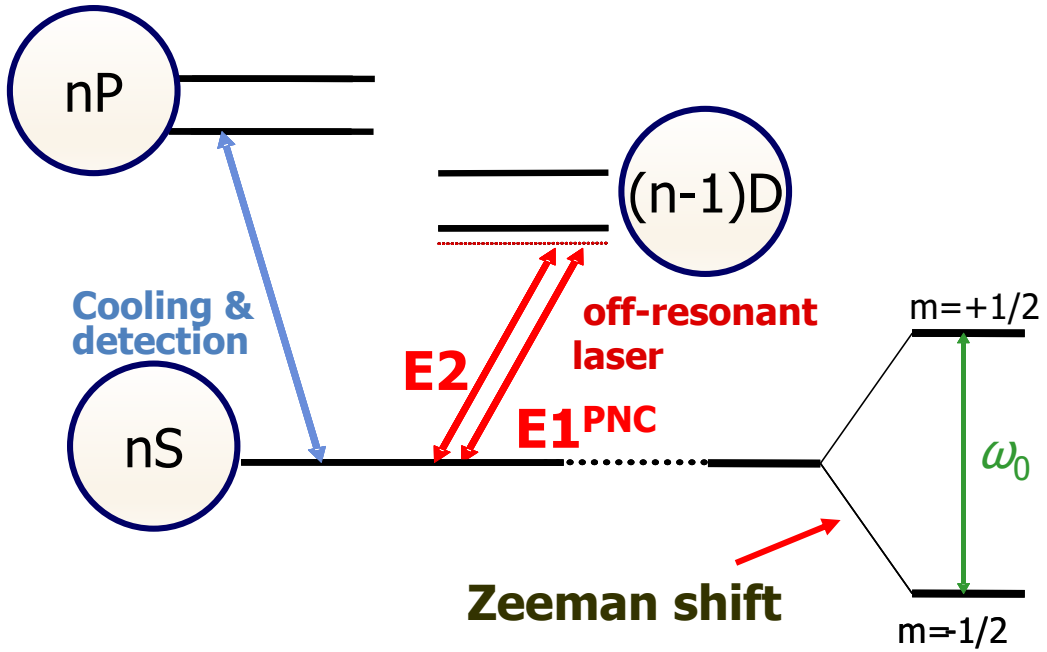

$$\left(\frac{E1_{PNC}^{NSI}}{Q_W}\right)^{theory} = \frac{\langle\Psi_f|D|\Psi_i\rangle}{\sqrt{\langle\Psi_f|\Psi_f\rangle\langle\Psi_i|\Psi_i\rangle}} \simeq \frac{\left[\left\langle\Psi_f^{(0)}\middle|D\middle|\Psi_i^{(1)}\right\rangle + \left\langle\Psi_f^{(1)}\middle|D\middle|\Psi_i^{(0)}\right\rangle\right]}{\sqrt{\left\langle\Psi_f^{(0)}\middle|\Psi_f^{(0)}\right\rangle\left\langle\Psi_i^{(0)}\middle|\Psi_i^{(0)}\right\rangle}}$$

Nuclear anapole moment

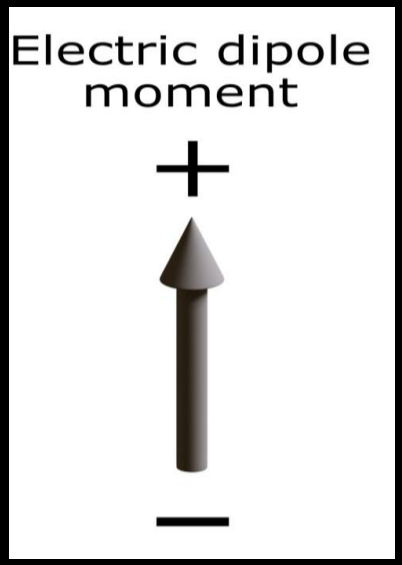

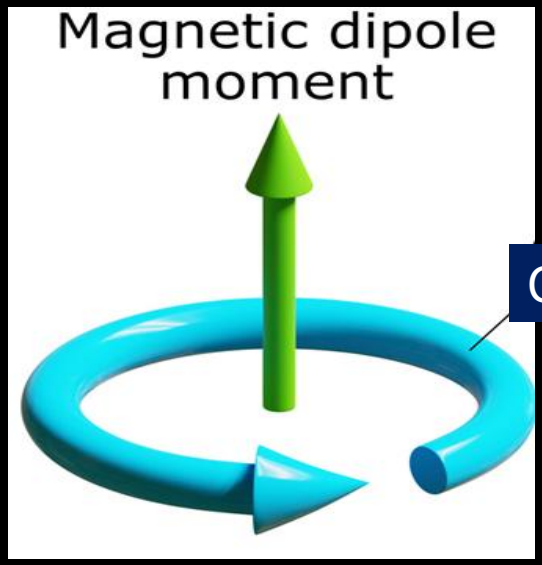

Current

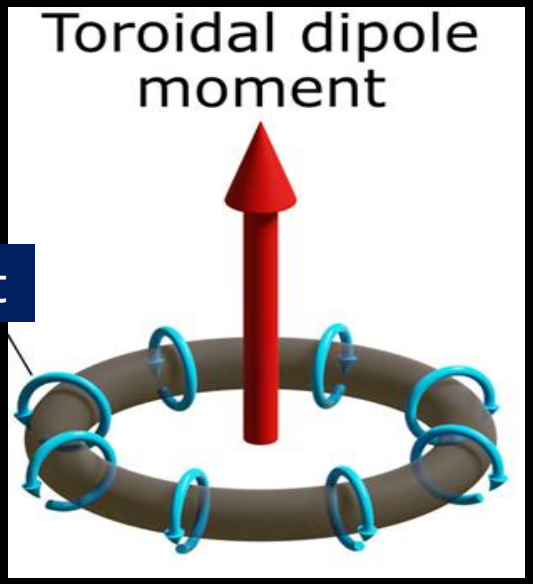

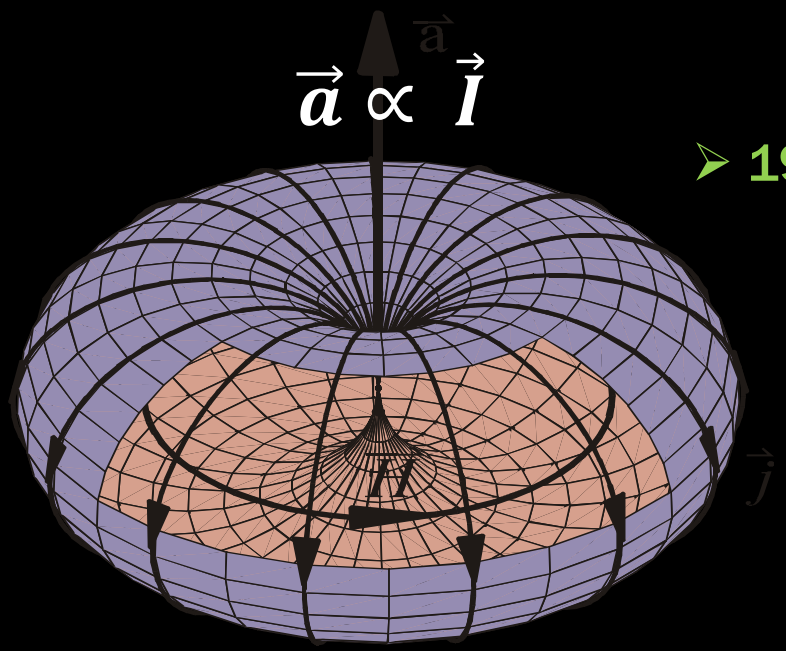

- **1959: Concept of Nuclear Anapole Moment:**
  (Ya. B. Zel'dovich & V. G. Vaks)

$$\kappa_a(^{133}Cs) = 0.102 \pm 0.0016$$

Chakraborty & Sahoo, Phys. Rev. A **110**, 022812 (2024).

CP/T-violation effects (EDMs) in Atom

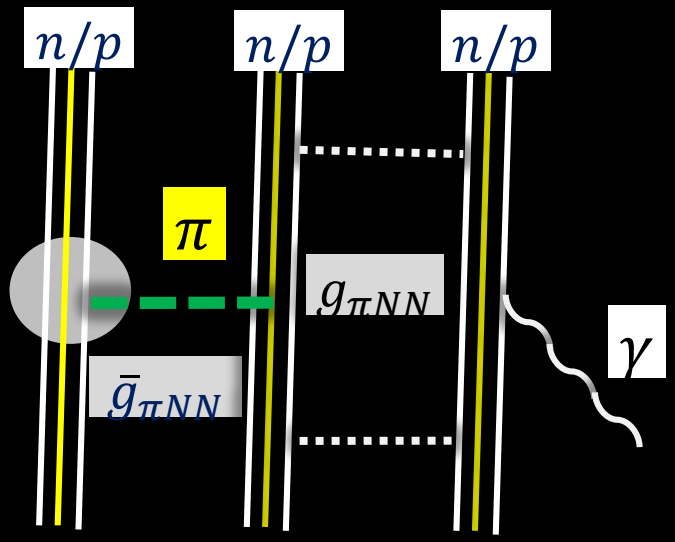

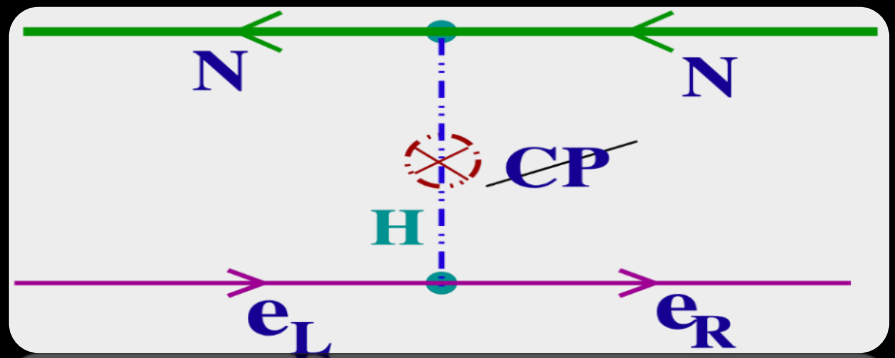

$$V_\chi(r,r') = \frac{e^{-m_\chi c|r-r'|}}{4\pi\,|r-r'|}$$

Electron size by the SM

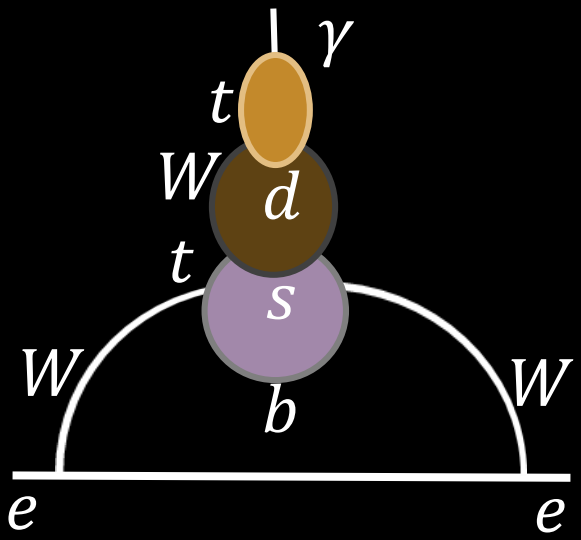

Electron size by the SUSY

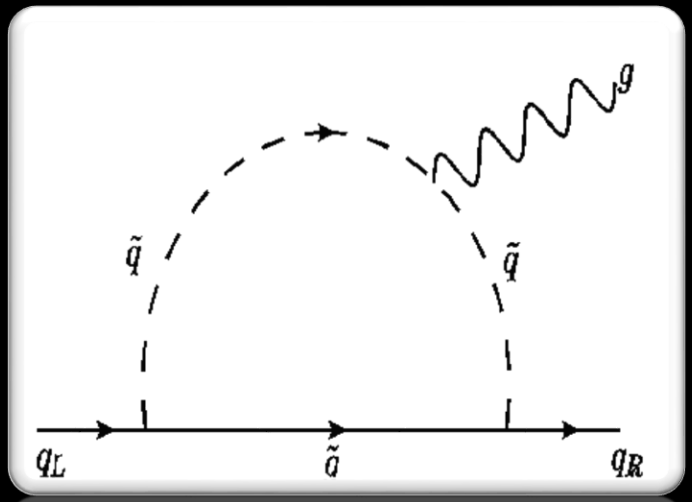

Atomic theory for EDM

EDM of a state $|\Psi_n\rangle$ given by: $D_a = \left[\frac{\langle\Psi_n|D|\Psi_n\rangle}{\langle\Psi_n|\Psi_n\rangle}\right]$

Mixed parity states: $|\Psi_n\rangle \simeq |\Psi_n^{(0)}\rangle + \lambda\,|\Psi_n^{(1)}\rangle$

$\mathrm{H} \equiv H_{at} + H_{EDM} = H_{at} + \lambda\, H_{odd}$ **with** $\lambda = S$ or $\langle\sigma_n\rangle C_T$

$$\Rightarrow D_a = \lambda\, R \cong 2\left[\frac{\langle\Psi_n^{(0)}|D|\Psi_n^{(1)}\rangle}{\langle\Psi_n^{(0)}|\Psi_n^{(0)}\rangle}\right]$$

Inhomogeneous Eq$^{\mathrm{n}}$:

$$(H_{at} - E_0^{(0)})|\Psi_n^{(1)}\rangle = -H_{EDM}|\Psi_n^{(0)}\rangle$$

Atomic Theory: in spherical coordinate system

Single particle solutions: Dirac equation: $h|\psi\rangle = \varepsilon\,|\psi\rangle$

with $h = c\,\vec{\alpha}\cdot\vec{p} + \beta m_e c^2 + V_N(r)$

Solution: $|\psi(r)\rangle = \frac{1}{r}\begin{pmatrix} P(r) & \mathrm{X}_{\kappa,m}(\theta,\phi) \\ iQ(r) & \mathrm{X}_{-\kappa,m}(\theta,\phi) \end{pmatrix}$

- Atomic states are described by ***n, J, π*** etc. quantum numbers.
- Purely spherical symmetric.

Two-body Coulomb interaction:

$$\frac{1}{|\vec{\mathbf{r}}_1 - \vec{\mathbf{r}}_2|} = \sum_{k,q} \frac{4\pi}{2k+1}\frac{r_<^k}{r_>^{k+1}}\,\mathbf{Y}_q^k(\theta,\phi)\cdot\mathbf{Y}_{-q}^{*k}(\theta,\phi)$$

Atomic system: Spherical symmetry

Schroedinger wave function: $|\phi_s(r)\rangle = \dfrac{R_{nl}(r)}{r} \mathrm{Y}_{l,m}(\theta,\phi)\sigma_s$

Hartree-Fock equation: $F\ C = S\ C\ \varepsilon$

$R_{nl}(r) = \sum_{i=1}^{N_l} c_{nl}^{i}\ |\zeta_i\rangle \quad \Rightarrow N_l \times N_l$ dimension matrix

Dirac wave function: $|\phi_D(r)\rangle = \dfrac{1}{r}\begin{pmatrix} P_{n\kappa}(r) & \mathrm{X}_{\kappa,m}(\theta,\phi) \\ iQ_{n\kappa}(r) & \mathrm{X}_{-\kappa,m}(\theta,\phi) \end{pmatrix}$

$P_{n\kappa}(r) = \sum_{i=1}^{N_\kappa} c_{n\kappa}^{i,L}\ |\zeta_i^L\rangle$ and $Q_{n\kappa}(r) = \sum_{i=1}^{N_\kappa} c_{n\kappa}^{i,S}\ |\zeta_i^S\rangle$

$$\Rightarrow \begin{pmatrix} F_{LL} & F_{LS} \\ F_{SL} & F_{SS} \end{pmatrix} \begin{pmatrix} C_{n\kappa}^{L} \\ C_{n\kappa}^{S} \end{pmatrix} = \begin{pmatrix} S_{LL} & 0 \\ 0 & S_{SS} \end{pmatrix} \begin{pmatrix} C_{n\kappa}^{L} \\ C_{n\kappa}^{S} \end{pmatrix} \varepsilon$$

$\Rightarrow 2N_\kappa \times 2N_\kappa$ dimension matrix

Bloch's prescription

According to the Bloch's prescription, the Fock space is divided into model (P) and orthogonal (Q) space.

$$H_0 = H_{DF} + \lambda V_{res} \quad |\Psi_0\rangle = \Omega \; |\Phi_0\rangle$$

$$P = |\Phi_0\rangle\langle\Phi_0| \quad \text{and} \quad Q = 1 - P$$

Fock space of H_{DF}

If energies of two systems **A** and **B**, and its combined system **AB** with **A** and **B** very far apart, computed in equivalent ways, satisfy

Size-consistency: $E(AB) = E(A) \oplus E(B)$

Size-extensitivity: $\Psi(AB) = \Psi(A) \otimes \Psi(B)$

Perturbation approach (MBPT)

$$H = H_0 + V_{int} \qquad |\Psi\rangle = \Omega \; | \Phi_0\rangle$$

$$P = |\Phi_0\rangle\langle\Phi_0| \qquad \text{and} \qquad Q = 1 - P$$

In perturbation approach:

$$\Omega = \Omega^{(0)} + \Omega^{(1)} + \Omega^{(2)} + \cdots = \sum_n \Omega^{(n)} \qquad \text{with} \quad \Omega^{(0)} = 1$$
$$E = E^{(0)} + E^{(1)} + E^{(2)} + \cdots = \sum_n E^{(n)}$$

Amplitude solving equation:

$$\left[\Omega^{(k)}, H_0\right] P = QV\, \Omega^{(k-1)} P - \sum_{m=1}^{(k-m)} PV_{int}\, \Omega^{(k-1)}\, P$$

Energy equation: $E^{(n)} = PV_{int}\Omega^{(n-1)}P$

Size-consistency problem with truncated MBPT

Brillouin-Wigner perturbation equation:

$$\left[\Omega^{(k)}, H_0\right]P = QV_{res}\,\Omega^{(k-1)}P - \sum_{m=1}^{(k-m)} \Omega^{(k-m)}PV_{res}\,\Omega^{(m-1)}\,P$$

$$= Q(H-E)\,\Omega^{(k-1)}P$$

This series converges faster, but has size-consistency problem.

Rayleigh-Schroedinger equation:

$$\left[\Omega^{(k)}, H_0\right]P = QV_{res}\,\Omega^{(k-1)}P - \sum_{m=1}^{(k-m)} \Omega^{(k-m)}PV_{res}\,\Omega^{(m-1)}\,P$$

$$= QV_{res}\,\Omega^{(k-1)}P - \sum_{m=1}^{k-1} \Omega^{(k-m)}E_0^{(m)}P$$

It does not converge faster, but avoids size-consistency problem.

Double sources of perturbation

In this case: $H = H_0 + V_{int}^{(1)} + V_{int}^{(2)}$

Let wave function is approximated as

$$|\Psi\rangle = |\Psi^{(0)}\rangle + |\Psi^{(\prime)}\rangle \approx |\Psi^{(0)}\rangle + |\Psi^{(1)}\rangle$$
$$E = E^{(0)} + E^{(\prime)} \approx E^{(0)}$$

In perturbation approach for this case:

$$\Omega = \Omega^{(0,0)} + \Omega^{(1,0)} + \Omega^{(0,1)} + \Omega^{(0,2)} + \Omega^{(1,1)} + \cdots = \sum_{n,m} \Omega^{(n,m)}$$

with $\Omega^{(0,0)} = 1$, $\Omega^{(1,0)} = V_{int}^{(1)}$ and $\Omega^{(0,1)} = V_{int}^{(2)}$

Amplitude equation:

$$\left[\Omega^{(\beta,\alpha)}, H_0\right]P = QV_{int}^{(1)}\Omega^{(\beta-1,\delta)}P + Q\,V_{int}^{(2)}\Omega^{(\beta,\delta-1)}P$$
$$- \sum_{m=1}^{\beta-1}\sum_{l=1}^{\delta-1}\left(\Omega^{(\beta-m,\delta-1)}PV_{int}^{(1)}\Omega^{(m-1,l)}P - \Omega^{(\beta-m,\delta-l)}PV_{int}^{(2)}\Omega^{(m,l-1)}P\right)$$

All-order many-body methods

$$|\Psi_0\rangle = \left|\Phi_0^{(0)}\right\rangle + \lambda_1 \left|\Phi_0^{(1)}\right\rangle + \lambda_1^2 \left|\Phi_0^{(2)}\right\rangle + \lambda_1^2 \left|\Phi_0^{(3)}\right\rangle + \cdots$$

Fock space — P-space — Q-space

i.e. $\left|\Phi_0^{(n)}\right\rangle = \sum_{k\neq 0}^{N} \left|\Phi_k^{(0)}\right\rangle C_{0k}^{(n)}$

In terms of level of excitations → Configuration Interaction (CI)

$$\Rightarrow |\Psi_0\rangle = \left|\Phi_0^{(0)}\right\rangle + C_I^{(\infty)} \left|\Phi_I^{(0)}\right\rangle + C_{II}^{(\infty)} \left|\Phi_{II}^{(0)}\right\rangle + \cdots$$

Further: $\left|\Phi_k^{(0)}\right\rangle \equiv \left|\Phi_{abc\ldots}^{pqr\ldots}\right\rangle = a_p^+ a_q^+ a_r^+ \ldots a_a a_b a_c \left|\Phi_0^{(0)}\right\rangle$

Coupled-cluster (CC) method:

$$\Rightarrow |\Psi_0\rangle = \left|\Phi_0^{(0)}\right\rangle + T_I \left|\Phi_0^{(0)}\right\rangle + \left(T_{II} + \frac{1}{2} T_I^2\right) \left|\Phi_0^{(0)}\right\rangle + \cdots + T_N \left|\Phi_0^{(0)}\right\rangle$$

$$= e^T \left|\Phi_0^{(0)}\right\rangle \qquad \text{where } T = T_I + T_{II} + \cdots + T_N$$

Approximated CI vs. CC methods

Configuration interaction (CI) method:

$$|\Psi_0\rangle = C_0|\Phi_0\rangle + C_I\,|\Phi_I\rangle + C_{II}\,|\Phi_{II}\rangle + \cdots + C_N\,|\Phi_N\rangle$$

Coupled-cluster (CC) method:

$$|\Psi_0\rangle = e^{T_I+T_{II}+\cdots+T_N}\,|\Phi_0\rangle = e^{T}|\Phi_0\rangle$$

Comparison between both:

$$C_0 \rightarrow 1$$

$$C_1 \rightarrow T_1$$

$$C_2 \rightarrow T_2 + \frac{1}{2}T_1^2$$

$$C_3 \rightarrow T_3 + T_1T_2 + \frac{1}{3!}T_1^3$$

so on …

Due to exponential ansatz, CCSD captures more correlation effects than CISD approximation.

Energy and amplitudes in (R)CC theory

Energy expression: $E_0 = \langle H_0 \rangle = \dfrac{\langle \Psi_0 | H_0 | \Psi_0 \rangle}{\langle \Psi_0 | \Psi_0 \rangle}$

$$E_0 = \frac{\langle \Phi_0 | e^{T^+} H_0 e^T | \Phi_0 \rangle}{\langle \Phi_0 | e^{T^+} e^T | \Phi_0 \rangle} = \frac{\sum_K \langle \Phi_0 | e^{T^+} e^T | \Phi_K \rangle \langle \Phi_K | e^{-T} H_0 e^T | \Phi_0 \rangle}{\langle \Phi_0 | e^{T^+} e^T | \Phi_0 \rangle}$$

$$= \langle \Phi_0 | e^{-T} H_0 e^T | \Phi_0 \rangle = \langle \Phi_0 | (H_0 e^T)_c | \Phi_0 \rangle$$

Excitation amplitudes: $\langle \Phi_K | (H_0 e^T)_c | \Phi_0 \rangle = 0$

It gets naturally terminated. Its appears in the form **A*X=B**; Jacobi iterative method is used.

RCC expressions for atomic properties

Property: $$\langle O\rangle = \frac{\langle\Psi_0|O|\Psi_0\rangle}{\langle\Psi_0|\Psi_0\rangle} = \frac{\langle\Phi_0|e^{T^+}Oe^{T}|\Phi_0\rangle}{\langle\Phi_0|e^{T^+}e^{T}|\Phi_0\rangle}$$

Matrix element evaluation expression:

$$\langle D\rangle_{fi} = \frac{\langle\Psi_f|D|\Psi_i\rangle}{\sqrt{\langle\Psi_f|\Psi_f\rangle\langle\Psi_i|\Psi_i\rangle}} = \frac{\langle\Phi_f|e^{T^+}De^{T}|\Phi_i\rangle}{\sqrt{\langle\Phi_f|e^{T^+}e^{T}|\Phi_f\rangle\langle\Phi_i|e^{T^+}e^{T}|\Phi_i\rangle}}$$

- Possesses two non-terminating series.
- Unmanageable with two-body operators like SMS operator.
- It does not satisfy the Hellmann-Feynman theorem.
- But any property can be evaluated.

All-order methods with external perturbation

Random phase approximation (RPA):

$$\left|\Psi_n^{(0)}\right\rangle \to |\Phi_n\rangle \qquad \text{and} \qquad \left|\Psi_n^{(1)}\right\rangle \to \Omega_{I,CP}^{(\infty,1)}|\Phi_n\rangle = \Omega_{RPA}^{(1)}|\Phi_n\rangle$$

Configuration interaction (CI) method:

$$\left|\Psi_n^{(0/1)}\right\rangle = C_0|\Phi_n\rangle + C_I\,|\Phi_I\rangle + C_{II}\,|\Phi_{II}\rangle + \cdots$$

Coupled-cluster (CC) method:

$$\begin{aligned}\left|\Psi_n^{(0/1)}\right\rangle &= C_0|\Phi_n\rangle + C_I\,|\Phi_I\rangle + C_{II}\,|\Phi_{II}\rangle + \cdots \\ &= |\Phi_n\rangle + T_I^{(0/1)}\,|\Phi_n\rangle + T_{II}^{(0/1)}\,|\Phi_n\rangle + \frac{1}{2}\,T_I^{(0/1)^2}|\Phi_n\rangle + \cdots \\ &= e^{T_I^{(0/1)}+T_{II}^{(0/1)}+\cdots}\,|\Phi_n\rangle = e^{T^{(0)}(+T^{(1)})}\,|\Phi_n\rangle\end{aligned}$$

Finite-field (FF) approach

Modified Hamiltonian: $H_\lambda = H_{at} + \lambda O$

$$E_\lambda = E_{at}^{(0)} + \lambda E_{at}^{(1)} + \lambda^2 E_{at}^{(2)} + \cdots$$

$$\langle O \rangle \equiv E_{at}^{(1)} \approx \left. \frac{\partial E_\lambda}{\partial \lambda} \right|_{\lambda \to 0}$$

$$\begin{pmatrix} Note: \lambda^2 \ terms \\ may \ not \ be \ small. \end{pmatrix}$$

- All the terms get naturally terminated.
- Not much additional computational costs required.
- Satisfies the Hellmann-Feynman theorem.
- Properties described by scalar operators can only be evaluated.
- Neglects $\mathfrak{O}(\lambda^2)$ contributions, which may not be small.
- Choice of λ depends on properties of interest ($\boldsymbol{F}$, $\boldsymbol{K}^{NMS}$, and $\boldsymbol{K}^{SMS}$ cannot be calculated accurately by considering same λ).

Analytic Response RCC method

In the AR RCC method, we express

$$H_\lambda = H_0 + \lambda O \quad \text{and} \quad |\Psi_0\rangle \simeq |\Psi_0^{(0)}\rangle + \lambda\,|\Psi_0^{(1)}\rangle$$

First-order eqn.: $(H_0 - E_0^{(0)})|\Psi_n^{(1)}\rangle = (E_0^{(1)} - O)\,|\Psi_0^{(0)}\rangle$

$$|\Psi_0\rangle = e^T|\Phi_0\rangle = e^{T^{(0)}+\lambda T^{(1)}}|\Phi_0\rangle$$

$$\Rightarrow \left|\Psi_0^{(0)}\right\rangle = \; e^{T^{(0)}}\,|\Phi_0\rangle$$

and $$\left|\Psi_0^{(1)}\right\rangle = \; e^{T^{(0)}}\left(1 + T^{(1)}\right)|\Phi_0\rangle$$

It yields that:

$$\langle O\rangle \equiv E_0^{(1)} = \langle\Phi_0\left|(H_0 e^{T^{(0)}}T^{(1)})_c + \left(O e^{T^{(0)}}\right)_c\right|\Phi_0\rangle$$

Advantages of AR RCC method

- All the terms are terminated.
- It does not satisfies the Hellmann-Feynman theorem.
- Any properties can be evaluated.
- Free from choice of any perturbative parameter.
- Computational efforts are less than the FF approach.

First development in atomic physics!!

Bi-orthogonal approach

In NCC: $|\Psi\rangle = e^{T}\,|\Phi_0\rangle$ and $\langle\tilde{\Psi}| = \langle\Phi_0|(1+\tilde{T})\,e^{-T}$

In ECC: $|\Psi\rangle = e^{T}\,|\Phi_0\rangle$ and $\langle\tilde{\Psi}| = \langle\Phi_0|e^{\tilde{T}}e^{-T}$

where T is a de-excitation operator similar to T^{+}.

This follows: $\langle\tilde{\Psi}|\Psi\rangle = \langle\Phi_0|e^{\tilde{T}}e^{-T}e^{T}|\Phi_0\rangle = 1.$

$$\langle O\rangle = \langle\tilde{\Psi}|O|\Psi\rangle = \langle\Phi_0|(Oe^{T})_c|\Phi_0\rangle + \langle\Phi_0|e^{\tilde{T}}(Oe^{T})_c|\Phi_0\rangle$$

B. K. Sahoo and B. P. Das, Phys. Rev. Letts. **120**, 203001 (2018).

- All the terms get naturally terminated.
- Satisfies the Hellmann-Feynman theorem.
- Any properties can be evaluated.
- Additional operators are introduced; computationally expensive.

Linear Response (R)CC method

$$H = H_0 + \varepsilon\, D \qquad \text{and} \qquad |\Psi_0\rangle \simeq |\Psi_0^{(0)}\rangle + \varepsilon\, |\Psi_0^{(1)}\rangle$$

First-order eqn.: $(H_0 - E_0^{(0)})|\Psi_n^{(1)}\rangle = (E_0^{(1)} - D)\ |\Psi_0^{(0)}\rangle$

$$|\Psi_0\rangle = e^{T}|\Phi_0\rangle = e^{T^{(0)}+\lambda T^{(1)}}|\Phi_0\rangle$$

$$\Rightarrow \left|\Psi_0^{(0)}\right\rangle = \ e^{T^{(0)}}\ |\Phi_0\rangle$$

and $$\left|\Psi_0^{(1)}\right\rangle = \ e^{T^{(0)}}\left(1 + T^{(1)}\right)|\Phi_0\rangle$$

It yields:

$$\boldsymbol{\alpha_d \simeq \langle \Phi_0 | e^{T^{(0)+}}\, D\, e^{T^{(0)}}\, T^{(1)} + T^{(1)+}\, e^{T^{(0)+}}\, D\, e^{T^{(0)}}\ |\Phi_0\rangle}$$

Tensor forms of any one- and two-body operators

Any one-body operator: $\langle JM|t^k_q|J'M'\rangle = (-1)^{J-M} \begin{pmatrix} J & k & J' \\ M & q & M' \end{pmatrix} \langle J||t^k||J''\rangle$

where $\langle J||t^k||J''\rangle$ Is the Mj-independent reduced matrix element.

Any two-body operator:

$$\langle J_1 M_1; J_2 M_2| \left[\mathbf{t}^{k_1}_{q_1}\mathbf{u}^{k_2}_{q_2}\right]^K_Q |J_1' M_1'\rangle = (-1)^{J_1-M_1+J_2-M_2} \begin{pmatrix} J_1 & k_1 & J_1' \\ M_1 & q_1 & M_1' \end{pmatrix} \begin{pmatrix} J_2 & k_2 & J_2' \\ M_2 & q_2 & M_2' \end{pmatrix}$$

$$\times \quad \langle J||[\mathbf{t}^{k_1}\mathbf{u}^{k_2}]^K||J'\rangle$$

where the two-body reduced matrix element:

$$\langle J||[\mathbf{t}^{k_1}\mathbf{u}^{k_2}]^K||J'\rangle = \sqrt{2K+1}\,(-1)^{J+J'+K} \sum_{J''} \langle J\left|\left|\mathbf{t}^{k_1}\right|\right|J''\rangle \ \langle J''\left|\left|\mathbf{u}^{k_2}\right|\right|J'\rangle \begin{Bmatrix} k_1 & k_2 & K \\ J' & J & J'' \end{Bmatrix}.$$

Using reduced matrix elements, we can use j-dependent basis instead of j,m_j-basis. However, it will introduce multipoles to the operators.

Selection rules for NSD PNC amplitudes

$$E1_{PNC}^{NSI(D)} = \frac{1}{\aleph}\left[\sum_{I\neq i}\frac{\left\langle \Psi_f^{(0)}\middle|D\middle|\Psi_I^{(0)}\right\rangle\left\langle \Psi_I^{(0)}\middle|H_{PNC}^{NSD}\middle|\Psi_i^{(0)}\right\rangle}{E_i^{(0)}-E_I^{(0)}} + \quad [f\leftrightarrow i]^{+}\right]$$

$$= \left[\left\langle J_f\middle|\left[D^{(1)}\otimes H_{PNC}^{(k)}\right]^{l}\middle|J_i\right\rangle + \left\langle J_f\middle|\left[H_{PNC}^{(k)}\otimes D^{(1)}\right]^{l}\middle|J_i\right\rangle\right]$$

Such that: $|J_f - j_i| \leq l \leq J_f + J_i$

Ranks of PNC Hamiltonians: NSI: $k = 0$ and NSD: $k = 1$

Thus:

$S_{1/2} \rightarrow S_{1/2}$ and $D_{3/2} \rightarrow S_{1/2}$ have both NSI and NSD contributions

But, $D_{5/2} \rightarrow S_{1/2}$ transition can have only the NSD contribution.

RCC operators in spherical coordinate system

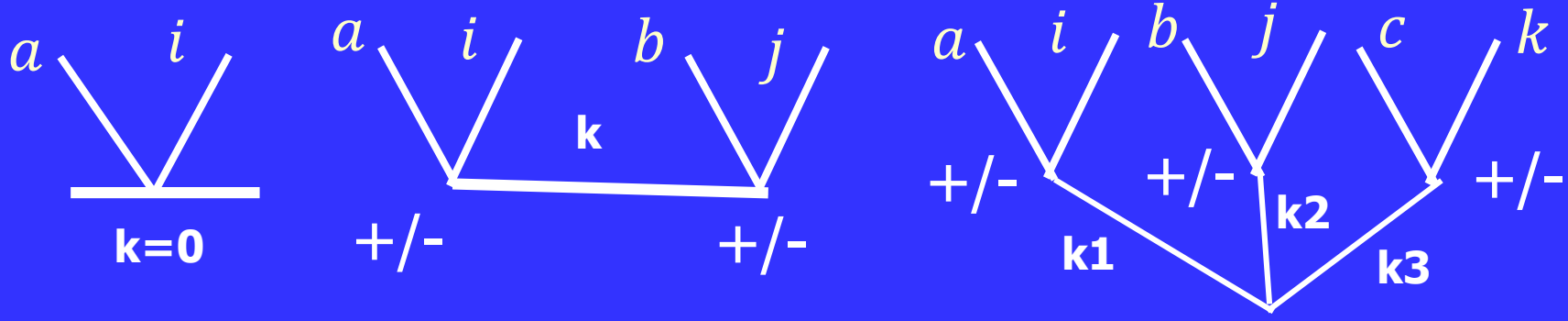

Unperturbed RCC operators: $T^{(0)} = T_1^{(0)} + T_2^{(0)} + T_3^{(0)} + \cdots$

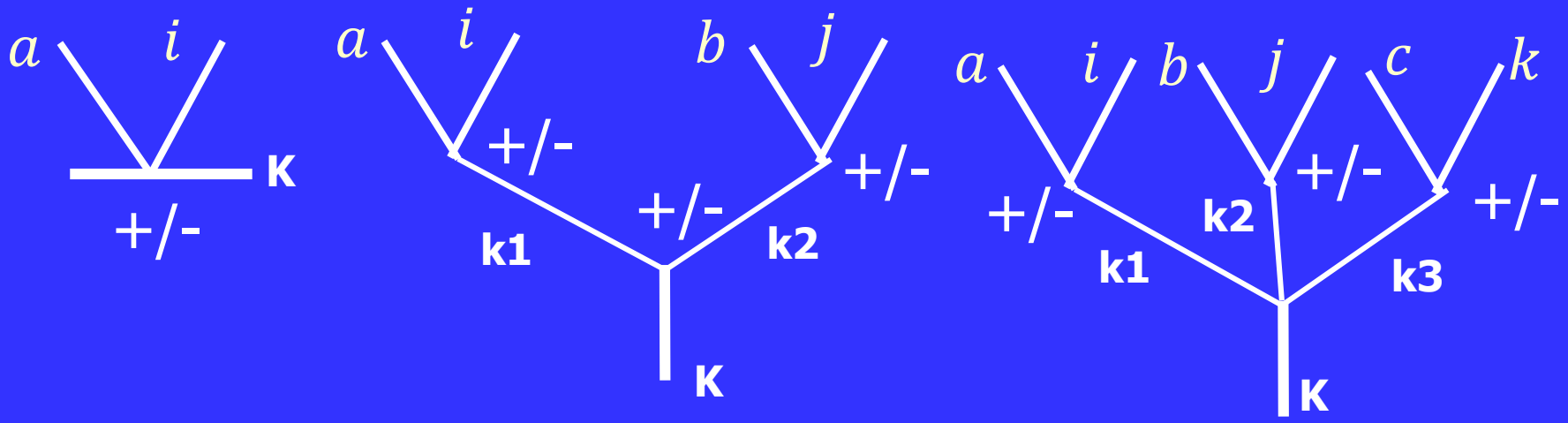

Perturbed RCC operators: $T^{(1)} = T_1^{(1)} + T_2^{(1)} + T_3^{(1)} + \cdots$

Choice of $V^{N-1/2}$ potentials: Fock-space approach

States of interest: $[5P^6]6S, [5P^6]7S, [5P^6]6P_{1/2}, [5P^6]7P_{1/2} \cdots\cdots$

Since $[5P^6]$ is common, its DF wave function ($|\Phi_0\rangle$) is obtained first, then for actual states are constructed as: $|\Phi_v\rangle = a_v^+|\Phi_0\rangle$. [$V^{N-1}$ potential]

In our RCC approach: $T \rightarrow T + S_v$

$$\Rightarrow \quad |\Psi_v\rangle = e^{T+S_v}\,|\Phi_v\rangle \equiv e^T(1+S_v)|\Phi_v\rangle$$
$$= a_v^+ e^T|\Phi_0\rangle + e^T S_v|\Phi_v\rangle = a_v^+|\Psi_0\rangle + |\Psi_v^{val}\rangle$$

Unperturbed states:

$$\left|\Psi_0^{(0)}\right\rangle = e^{T^{(0)}}|\Phi_0\rangle \quad \text{and} \quad \left|\Psi_v^{(0)}\right\rangle = e^{T^{(0)}}\left(1+S_v^{(0)}\right)|\Phi_v\rangle$$

First-order states:

$$\left|\Psi_0^{(1)}\right\rangle = e^{T^{(0)}}\left(1+T^{(1)}\right)|\Phi_0\rangle \quad \text{and} \quad \left|\Psi_v^{(1)}\right\rangle = e^{T^{(0)}}\left(S_v^{(1)} + T^{(1)}(1+S_v^{(0)})\right)|\Phi_v\rangle$$

Similarly it can be extended to two-valence systems:

Equation-of-motion CC method

Ground state: $|\Psi_0\rangle = e^T|\Phi_0\rangle$

Excited state with definite J and π:

$$|\Psi_K(J,\pi)\rangle = R_K(J,\pi)|\Psi_0\rangle = R_K(J,\pi)e^T|\Phi_0\rangle$$

Here $R_K(J,\pi) = r_0 + R_1(J,\pi) + R_2(J,\pi) + \cdots$

Equation of motion: $H|\Psi_K(J,\pi)\rangle = E_K|\Psi_K(J,\pi)\rangle$

$$\Rightarrow \left(He^T\right)_c R_K(J,\pi)|\Phi_0\rangle = (E_K - E_0)R_K(J,\pi)|\Phi_0\rangle$$

And, $\langle\widetilde{\Psi}_K(J,\pi)| = \langle\widetilde{\Psi}_0|L_K(J,\pi)$ with $L_K(J,\pi) = l_0 + L_1(J,\pi) + \cdots$

Amplitude solving equations for R_K (similar for L_K):

$$\left[\begin{pmatrix} P(He^T)_c P & P(He^T)_c Q \\ Q(He^T)_c P & Q(He^T)_c Q \end{pmatrix}\begin{pmatrix} r_0 P \\ QR_K P \end{pmatrix}\right]_c = \Delta E_K \begin{pmatrix} r_0 P \\ QR_K P \end{pmatrix}.$$

Comparative Analysis of Mg^+ Properties using Multiconfiguration Dirac-Hartree-Fock and Relativistic Coupled-cluster Methods

B. K. Sahoo *
Atomic, Molecular and Optical Physics Division, Physical Research Laboratory, Navrangpura, Ahmedabad 380009, India

Per Jönsson †
Malmö University, Faculty of Technology and Society (TS), Department of Materials Science and Applied Mathematics (MTM)

Gediminas Gaigalas
Institute of Theoretical Physics and Astronomy, Faculty of Physics, Vilnius University, Saulėtekio Ave. 3, LT-10257 Vilnius, Lithuania

(Submitted)

TABLE II. Calculated excitation energies (in cm^{-1}) at different layers using the MCDHF/RCI method. The final results from the MCDHF/RCI method are taken from the "layer 7" along with some corrections from the triple excitations (layer 7+T) and they are compared with the experimental values from the NIST ASD database [36]. NCSFs is the total number of CSFs in the wave function expansion.

State	layer 1	layer 2	layer 3	layer 4	layer 5	layer 6	layer 7	layer 7+T	Experiment
$3s\ ^2S_{1/2}$	0	0	0	0	0	0	0	0	0
$3p\ ^2P^o_{1/2}$	35742.44	35648.53	35555.39	35547.24	35545.12	35544.12	35544.13	35576.67	35669.31
$3p\ ^2P^o_{3/2}$	35839.13	35739.69	35646.15	35637.97	35635.92	35634.91	35635.04	35667.68	35760.88
$4s\ ^2S_{1/2}$	69521.77	69662.64	69624.34	69632.30	69632.43	69633.29	69631.99	69662.40	69804.95
$3d\ ^2D_{3/2}$	71139.14	71324.45	71291.88	71303.64	71307.31	71307.54	71308.06	71346.15	71491.06
$3d\ ^2D_{5/2}$	71139.72	71325.37	71292.77	71304.50	71308.17	71308.38	71308.91	71347.01	71490.19
$4p\ ^2P^o_{1/2}$	80381.37	80482.75	80416.93	80422.22	80422.21	80423.02	80421.92	80460.44	80619.50
$4p\ ^2P^o_{3/2}$	80414.13	80513.16	80447.19	80452.48	80452.49	80453.30	80452.24	80490.79	80650.02
NCSFs	313875	633060	1141855	1887910	2852859	3912274	5141775	25605619	

TABLE III. Calculated second ionization potential and excitation energies (in cm^{-1}) at different levels of approximation in the RCC theory and comparison with the experimental values [36].

State	DHF	RCCSD	RCCSDT	Basis	Breit	QED	Final	Experiment
Second ionization potential								
$3s\ ^2S_{1/2}$	118823.96	121182.36	121250.59	14.15	−8.13	−8.09	121249(15)	121267.64
Excitation energies								
$3p\ ^2P^o_{1/2}$	34530.15	35631.66	35659.64	4.99	0.53	−8.91	35656(20)	35669.31
$3p\ ^2P^o_{3/2}$	34620.49	35729.20	35757.28	5.05	−4.85	−8.65	35749(20)	35760.88
$4s\ ^2S_{1/2}$	67967.16	69739.45	69792.55	10.68	−5.83	−5.89	69792(18)	69804.95
$3d\ ^2D_{3/2}$	69482.97	71427.61	71485.35	6.73	−8.60	−8.09	71475(18)	71491.06
$3d\ ^2D_{5/2}$	69482.14	71426.88	71484.59	6.74	−8.61	−8.08	71475(18)	71490.19
$4p\ ^2P^o_{1/2}$	78576.27	80549.97	80606.04	11.27	−5.16	−8.37	80604(16)	80619.50
$4p\ ^2P^o_{3/2}$	78606.96	80582.51	80638.62	11.28	−6.99	−8.28	80635(16)	80650.02

Comparative Analysis of Mg^+ Properties using Multiconfiguration Dirac-Hartree-Fock and Relativistic Coupled-cluster Methods

B. K. Sahoo *
Atomic, Molecular and Optical Physics Division, Physical Research Laboratory, Navrangpura, Ahmedabad 380009, India

Per Jönsson †
Malmö University, Faculty of Technology and Society (TS), Department of Materials Science and Applied Mathematics (MTM)

Gediminas Gaigalas
Institute of Theoretical Physics and Astronomy, Faculty of Physics, Vilnius University, Saulėtekio Ave. 3, LT-10257 Vilnius, Lithuania

(Submitted)

Atomic State $\|\Psi_i\rangle$	Decay State $\|\Psi_f\rangle$	BR Γ	Lifetime (in ns) MCDHF /RCI	RCC	Experiment
$3p\ ^2P^o_{1/2}$	$\rightarrow 3s\ ^2S_{1/2}$	1.0	3.889	3.879(7)	3.854(30) [42] 4.0(3) [43] 6.20(38) [44] 4.2(4) [45] 4.5(8) [46]
$3p\ ^2P^o_{3/2}$	$\rightarrow 3s\ ^2S_{1/2}$	1.0	3.859	3.844(7)	3.810(40) [42] 4.0(3) [43] 6.20(38) [44] 4.2(4) [45] 4.5(8) [46]
$4s\ ^2S_{1/2}$	$\rightarrow 3p\ ^2P^o_{3/2}$	0.67	2.898	2.883(2)	2.6(3) [43] 2.8(4) [45] 3.8(5) [46]
	$\rightarrow 3p\ ^2P^o_{1/2}$	0.33			
$3d\ ^2D_{5/2}$	$\rightarrow 3p\ ^2P^o_{3/2}$	1.0	2.081	2.079(2)	2.2(2) [43] 1.9(2) [45] 2.3(4) [46]
$3d\ ^2D_{3/2}$	$\rightarrow 3p\ ^2P^o_{3/2}$	0.17	2.073	2.071(2)	2.2(2) [43] 1.9(2) [45] 2.3(4) [46]
	$\rightarrow 3p\ ^2P^o_{1/2}$	0.83			
$4p\ ^2P^o_{1/2}$	$\rightarrow 3d\ ^2D_{3/2}$	0.30	18.566	18.462(26)	21(2) [43]
	$\rightarrow 4s\ ^2S_{1/2}$	0.67			
	$\rightarrow 3s\ ^2S_{1/2}$	0.03			
$4p\ ^2P^o_{3/2}$	$\rightarrow 3d\ ^2D_{3/2}$	0.03	18.480	18.411(27)	21(2) [43]
	$\rightarrow 3d\ ^2D_{5/2}$	0.28			
	$\rightarrow 4s\ ^2S_{1/2}$	0.67			
	$\rightarrow 3s\ ^2S_{1/2}$	0.02			

TABLE VIII. Contributions from different E1 matrix elements from the MCDHF/RCI and RCC methods to the ground state electric dipole polarizability (in a.u.) of Mg^+. The tail, core-valence and core contributions are estimated using the RPA. The final values from both the MCDHF/RCI and RCC methods are compared with the values previously obtained using other methods and experiment.

Reference	Source	MCDHF/RCI	RCC
This work			
	$3p\ ^2P^o_{1/2}$	11.59	11.50(2)
	$3p\ ^2P^o_{3/2}$	23.12	22.97(4)
	$4p\ ^2P^o_{1/2}$	~ 0.0	$\sim 0.0(1)$
	$4p\ ^2P^o_{3/2}$	0.01	0.01(1)
	Tail	0.02(2)	
	Core-valence	−0.02(2)	
	Core	0.44(4)	
	Final	35.16	34.92(7)
Experiment		$33.80^{+0.50}_{-0.30}$	[58]

Comparative Analysis of Mg^+ Properties using Multiconfiguration Dirac-Hartree-Fock and Relativistic Coupled-cluster Methods

B. K. Sahoo *
Atomic, Molecular and Optical Physics Division, Physical Research Laboratory, Navrangpura, Ahmedabad 380009, India

Per Jönsson †
Malmö University, Faculty of Technology and Society (TS), Department of Materials Science and Applied Mathematics (MTM)

Gediminas Gaigalas
Institute of Theoretical Physics and Astronomy, Faculty of Physics, Vilnius University, Saulėtekio Ave. 3, LT-10257 Vilnius, Lithuania

(Submitted)

TABLE IX. The calculated A_{hf} values (in MHz) at different layers using the MCDHF/RCI method. The final results from the MCDHF/RCI method are taken from the "layer 7" along with some corrections from the triple excitations (layer 7+T), and they are compared with the experimental values.

State	layer 1	layer 2	layer 3	layer 4	layer 5	layer 6	layer 7	layer 7+T	Experiment
$3s\ ^2S_{1/2}$	−556.71	−567.85	−575.60	−576.21	−589.28	−589.40	−589.82	−592.48	−596.2542487(42) [59]
									−596.2544(5) [60]
$3p\ ^2P^o_{1/2}$	−97.68	−98.44	−100.17	−100.60	−101.11	−101.12	−101.36	−101.81	
$3p\ ^2P^o_{3/2}$	−20.61	−20.71	−19.26	−19.21	−18.69	−18.69	−18.79	−18.97	
$4s\ ^2S_{1/2}$	−150.82	−153.51	−156.78	−157.62	−161.21	−161.26	−161.36	−162.16	
$3d\ ^2D_{3/2}$	−1.19	−1.15	−1.14	−1.14	−1.13	−1.14	−1.14	−1.13	
$3d\ ^2D_{5/2}$	0.17	0.071	0.055	0.046	0.032	0.033	0.035	0.071	
$4p\ ^2P^o_{1/2}$	−32.32	−32.37	−33.02	−33.35	−33.55	−33.55	−33.63	−33.80	
$4p\ ^2P^o_{3/2}$	−6.68	−6.76	−6.27	−6.30	−6.13	−6.13	−6.16	−6.22	

TABLE X. The calculated A_{hf} values (in MHz) of $^{25}Mg^+$ at different levels of approximation in the RCC theory and comparison with the experimental values. The corrections from Basis, BW, Breit, and QED are given from the RCCSD method. The final results include RCCSDT values with other corrections.

State	DHF	RCCSD	RCCSDT	Basis	BW	Breit	QED	Final	Experiment
$3s\ ^2S_{1/2}$	−462.70	−595.70	−597.97	−0.27	0.30	−0.31	1.63	−596.6(8)	−596.2542487(42) [59]
									−596.2544(5) [60]
$3p\ ^2P^o_{1/2}$	−76.96	−102.53	−103.31	−0.03	~ 0.0	−0.02	~ 0.0	−103.4(5)	
$3p\ ^2P^o_{3/2}$	−15.24	−19.12	−19.29	−0.01	~ 0.0	−0.01	~ 0.0	−19.31(5)	
$4s\ ^2S_{1/2}$	−130.33	−163.22	−163.61	−0.06	0.08	−0.01	0.42	−163.2(6)	
$3d\ ^2D_{3/2}$	−1.26	−1.16	−1.15	~ 0.0	~ 0.0	~ 0.0	~ 0.0	−1.15(3)	
$3d\ ^2D_{5/2}$	−0.54	0.10	0.14	~ 0.0	~ 0.0	0.01	~ 0.0	0.15(2)	
$4p\ ^2P^o_{1/2}$	−26.15	−34.09	−34.40	−0.01	~ 0.0	−0.01	~ 0.0	−34.42(8)	
$4p\ ^2P^o_{3/2}$	−5.18	−6.28	−6.32	−0.01	~ 0.0	~ 0.0	~ 0.0	−6.33(5)	

Comparative Analysis of Mg^+ Properties using Multiconfiguration Dirac-Hartree-Fock and Relativistic Coupled-cluster Methods

B. K. Sahoo *
Atomic, Molecular and Optical Physics Division, Physical Research Laboratory, Navrangpura, Ahmedabad 380009, India

Per Jönsson †
Malmö University, Faculty of Technology and Society (TS), Department of Materials Science and Applied Mathematics (MTM)

Gediminas Gaigalas
Institute of Theoretical Physics and Astronomy, Faculty of Physics, Vilnius University, Saulėtekio Ave. 3, LT-10257 Vilnius, Lithuania

(Submitted)

TABLE XVIII. Recommended IS constants of low-lying transitions in Mg^+ from the RCC theory.

	F values (in MHz/fm^2)		K^{NMS} values (in GHz amu)		K^{SMS} values (in GHz amu)	
Transition	This work	Experiment	This work	Scaling	This work	Experiment
$3s\ ^2S_{1/2} \rightarrow 3p\ ^2P^o_{1/2}$	−126(1)	−127(12)	586(2)	586.59	366(5)	369.3(3)
$3s\ ^2S_{1/2} \rightarrow 3p\ ^2P^o_{3/2}$	−126(1)		587(2)	588.09	367(5)	367.7(3)
$3s\ ^2S_{1/2} \rightarrow 4s\ ^2S_{1/2}$	−85(1)		1147(1)	1147.98	19(2)	
$3s\ ^2S_{1/2} \rightarrow 3d\ ^2D_{3/2}$	−116(1)		1174(1)	1175.70	166(5)	
$3s\ ^2S_{1/2} \rightarrow 3d\ ^2D_{5/2}$	−116(1)		1174(1)	1175.71	167(5)	
$3s\ ^2S_{1/2} \rightarrow 4p\ ^2P^o_{1/2}$	−120(1)		1324(1)	1325.84	164(5)	
$3s\ ^2S_{1/2} \rightarrow 4p\ ^2P^o_{3/2}$	−120(1)		1325(1)	1326.34	165(5)	

TABLE XIX. IS constants of low-lying transitions in Mg^+ from RCI

	F values (in MHz/fm^2)		K^{NMS} values (in GHz amu)		K^{SMS} values (in GHz amu)	
Transition	SD	SDT	SD	SDT	SD	SDT
$3s\ ^2S_{1/2} \rightarrow 3p\ ^2P^o_{1/2}$	−125	−125	613	596	304	321
$3s\ ^2S_{1/2} \rightarrow 3p\ ^2P^o_{3/2}$	−125	−125	614	597	304	321
$3s\ ^2S_{1/2} \rightarrow 4s\ ^2S_{1/2}$	−84.5	−84.1	1205	1162	−75	−54
$3s\ ^2S_{1/2} \rightarrow 3d\ ^2D_{3/2}$	−116	−116	1249	1196	55	87
$3s\ ^2S_{1/2} \rightarrow 3d\ ^2D_{5/2}$	−116	−116	1249	1196	55	88
$3s\ ^2S_{1/2} \rightarrow 4p\ ^2P^o_{1/2}$	−119	−119	1387	1342	58	84
$3s\ ^2S_{1/2} \rightarrow 4p\ ^2P^o_{3/2}$	−119	−119	1387	1342	58	84

Summary and Outlook

- Developed all-order relativistic coupled-cluster methods for accurate calculations of atomic properties.
- Methods are developed in the FF, EVE and AR frameworks to estimate isotope shift constants.
- Linear response approach is developed for polarizability calculations.
- Bi-orthogonal method is developed only for the ground state properties of closed-shell systems.

Methods yet to be developed:

- **Bi-orthogonal approach for the open-shell system**
- **Analytical response approach for hyperfine structure constants**
- **Equation-of-motion approach for excited states**
- **Focks-space approach for two-valence systems**

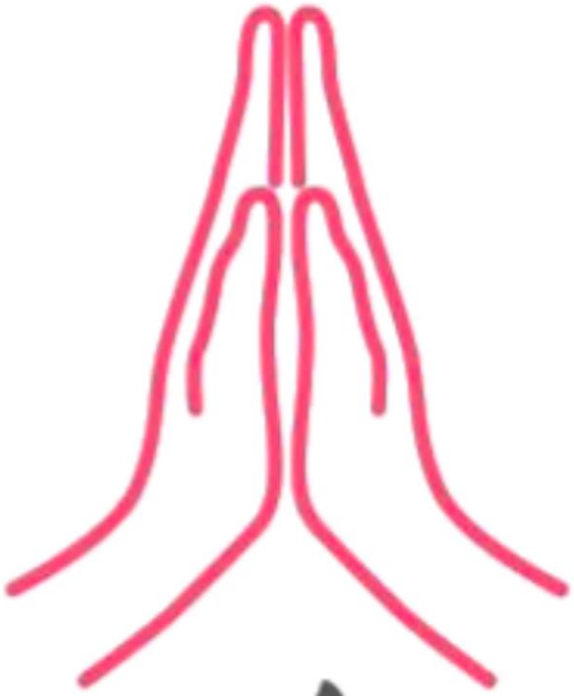

Thank you.